Current Research in Toxicology 5 (2023) 100132

Contents lists available at ScienceDirect

Current Research in Toxicology

journal homepage: www.journals.elsevier.com/current-research-in-toxicology

Proximal tubular transport of Metallothionein-Mercury complexes and protection against nephrotoxicity

Aditi Dave [a], Lucy Joshee [a], Delon W. Barfuss [c], Ryan Brownlee [a], Roha Surani [a], Sahar Anis Ali [a], Earl G. Ford IV [a], Elizabeth G. Pittman [a], Anasalea V.G. Caroland [a], Jennifer Barkin [b], Christy C. Bridges [a,*]

[a] Department of Biomedical Sciences, Mercer University School of Medicine, Macon, GA, USA
[b] Department of Community Medicine, Mercer University School of Medicine, Macon, GA, USA
[c] Department of Biology, Georgia State University, Atlanta, GA, USA

ARTICLE INFO

Keywords:
Mercury
Metallothionein
Kidney
Nephrotoxicity
Heavy metals

ABSTRACT

Mercury (Hg) is an important environmental toxicant to which humans are exposed on a regular basis. Mercuric ions within biological systems do not exist as free ions. Rather, they are bound to free sulfhydryl groups (thiols) on biological molecules. Metallothionein (MT) is a cysteine-rich, metal-binding protein that has been shown to bind to heavy metals and reduce their toxic effects in target cells and organs. Little is known about the effect of MT on the handing and disposition of Hg. Therefore, the current study was designed to test the hypothesis that overexpression of MT alters the corporal disposition of Hg and reduces its nephrotoxicity. Furthermore, the current study examined the transport of Hg-MT complexes in isolated proximal tubules. Rats were treated with saline or Zn followed by injection with a non-nephrotoxic (0.5 μmol kg^{-1}), moderately nephrotoxic (1.5 μmol kg^{-1}), or significantly nephrotoxic (2.25 μmol kg^{-1}) dose of $HgCl_2$ (containing radioactive Hg). Pretreatment with Zn increased mRNA expression of MT and enhanced accumulation of Hg in the renal cortex of male and female rats. In addition, injection with Zn also protected animals from Hg-induced nephrotoxicity. Studies using isolated proximal tubules from rabbit kidney demonstrated that Hg-MT is taken up rapidly at the apical and basolateral membranes. The current findings suggest that at least part of this uptake occurs through an endocytic process. This study is the first to examine the uptake of Hg-MT complexes in isolated proximal tubules. Overall, the findings of this study suggest that supplementation with Zn may be a viable strategy for reducing the risk of Hg intoxication in at-risk populations.

Introduction

Mercury is a prevalent environmental toxicant that is recognized by the World Health Organization as one of the top 10 metals of public health concern (WHO, 2020). It is released into the environment through natural sources or anthropogenic activities, following which, it is deposited in soil and bodies of water throughout the world. Owing to this, humans are exposed to Hg on a regular basis. The majority of human exposure results from the consumption of fish and other aquatic organisms that are contaminated with organic forms of mercury (e.g., methylmercury). Humans may also be exposed to mercury vapor through mining and other occupational activities. Interestingly, once ingested and absorbed into the circulation, methylmercury and mercury vapor can be biotransformed to inorganic mercury (Hg^{2+}) (Norseth and Clarkson, 1970a, b). Because of this transformation, the current study examined the disposition and toxicity of Hg^{2+} under various experimental conditions. Furthermore, since the kidney is the primary site of accumulation and toxicity of Hg^{2+}, the current study focused on the renal handling and disposition of Hg^{2+}.

It is important to note that mercuric ions have a strong affinity for free sulfhydryl (-SH) groups. Once mercuric ions are absorbed into the circulation, they bind to free sulfhydryl groups on biomolecules such as albumin, cysteine, and glutathione (Bridges and Zalups, 2017). Metallothioneins (MT) are small cysteine-containing, metal-binding proteins

Abbreviations: Hg, mercury; Hg^{2+}, inorganic mercury; MT, metallothionein; OSOM, outer stripe of outer medulla; Zn, zinc; GSH, glutathione; MURR, University of Missouri Research Reactor; DMPS, 2,3-dimercapto-1-propanesulfonic acid.

* Corresponding author at: 1550 College St., Macon, GA 31207, USA.
E-mail address: Bridges_cc@mercer.edu (C.C. Bridges).

https://doi.org/10.1016/j.crtox.2023.100132
Received 24 July 2023; Received in revised form 25 September 2023; Accepted 11 October 2023
Available online 20 October 2023

that are found in a variety of tissues and organs (Nordberg and Nordberg, 2022). Four major isoforms (MT1 – MT4), along with numerous sub-isoforms, have been identified in mammals (Merlos Rodrigo et al., 2020). MT1 and MT2 have been identified in many tissues and are particularly prevalent in the liver and kidneys (Merlos Rodrigo et al., 2020). MT isoforms are present in the cytoplasm, lysosomes, mitochondria, and nuclei of mammalian cells (Sabolic et al., 2018). They have several important functions, including storage and transport of intracellular metals, protection against metal toxicity, scavenging free radicals, and cell repair (Sabolic et al., 2018).

Numerous studies have shown that exposure to heavy metals, such as cadmium, zinc, and Hg, upregulates the expression of MT (Nordberg and Nordberg, 2022; Zalups and Koropatnick, 2000). It has been proposed that cadmium in blood binds to MT, following which, it is delivered to the glomerulus for filtration and excretion (Nordberg and Nordberg, 2022). In contrast, little is known about MT and its interaction with Hg. Therefore, the current study was designed to test the hypothesis that induction of MT alters the disposition of Hg and reduces Hg-induced nephrotoxicity. Additionally, since the expression of mRNA encoding MT has been shown to be 2–3-fold greater in female rats than in males (Sabolic et al., 2018), the current study also compared the effects of MT on the handling of Hg in male and female rats.

Methods

2.1. Animals

Male (n = 28) and female (n = 28) Wistar rats, weighing 225–250 g, were obtained from our in-house breeding colony housed in the Mercer University School of Medicine animal facility. Male (n = 3) and female (n = 3) New Zealand White rabbits were also obtained from our in-house breeding colony. Animals were provided a commercial laboratory diet (Envigo) and water *ad libitum* throughout all aspects of the present study. All procedures involving animals were reviewed and approved by the Mercer University Institutional Animal Care and Use Committee. Animals were handled in accordance with the Guide for the Care and Use of Laboratory Animals as adopted by the National Institutes of Health.

2.2. Radioactive mercury

Radioactive mercury ([^{203}Hg]) was generated according to our previously published protocol (Belanger et al., 2001; Bridges et al., 2004). Briefly, 3 mg of mercuric oxide (87 % enriched ^{202}Hg; Trace Sciences) was irradiated for four weeks at the University of Missouri Research Reactor (MURR). The radioactive Hg was dissolved in 1 mL of 1 N HCl and stored at −20 °C. Specific activities ranged from 8 to 12 mCi/mg.

2.3. Injections

Each group of male and female rats was divided into two groups of 14 rats and injected intraperitoneally with saline or 25 mg/kg zinc sulfate (Zn). Twenty-four h after Zn injection, two saline-injected and two Zn-injected rats were euthanized to serve as controls. The remaining 12 rats were divided into groups of four and were injected intravenously (i.v.) with either a non-nephrotoxic dose (0.5 μmol • kg^{-1} • 2 mL^{-1} normal saline), a moderately nephrotoxic dose (1.5 μmol • kg^{-1} • 2 mL^{-1} normal saline) or a significantly nephrotoxic dose of $HgCl_2$ (2.25 μmol • kg^{-1} • 2 mL^{-1} normal saline) according to our previously published protocol (Bridges et al., 2008a; Bridges et al., 2015). The injection solution contained radioactive mercury ([^{203}Hg]) and was designed to deliver 1 μCi [^{203}Hg] to each animal. (Bridges et al., 2008a). At the time of injection, each animal was anesthetized with isoflurane and a small incision was made in the skin in the mid-ventral region of the thigh to expose the femoral vein and artery. A 0.5-μmol, 1.5-μmol or 2.5-μmol • kg^{-1} dose of $HgCl_2$ was administered into the vein. The wound was closed using two 9-mm stainless steel wound clips. Animals were then housed individually in metabolic cages. Twenty-four hours after injection with $HgCl_2$, animals were sacrificed and organs and tissues were harvested.

2.4. Collection of organs

At the time of euthanasia, animals were anesthetized with an intraperitoneal injection of ketamine (70 mg • kg^{-1}) and xylazine (30 mg • kg^{-1}). A 1-mL sample of blood was obtained from the inferior vena cava for determination of [^{203}Hg] content. A separate sample of blood was placed in a Microtainer plasma separation tube in order to estimate content of [^{203}Hg] in plasma and cellular fractions. The total volume of blood was estimated to be 6 % of body weight (Lee and Blaufox, 1985).

The kidneys and liver were also removed from each rat. Each kidney was trimmed of fat and fascia, weighed, and cut in half along the mid-traverse plane. One-half of the right kidney was placed in fixative (40 % formaldehyde, 50 % glutaraldehyde in 96.7 mM NaH_2PO_4 and 67.5 mM NaOH) in preparation for histological analyses. The remaining half was frozen in liquid nitrogen for future RNA analyses. One-half of the left kidney was utilized for estimation of [^{203}Hg] content. A 3-mm traverse slice was obtained from the remaining half and was used for dissection of renal zones (cortex, outer stripe of the outer medulla (OSOM), inner stripe of the outer medulla, and inner medulla). Each sample was weighed and placed in a separate tube for estimation of [^{203}Hg]. The liver was weighed, and a 1-g sample was removed for determination of [^{203}Hg] content.

Urine and feces were collected during the 24-h period after Hg injection. The total volume of urine was measured, and a 1-mL sample was collected and placed in a tube for estimation of [^{203}Hg] content. All of the feces excreted after injection with Hg were counted for estimation of [^{203}Hg] content. The content of [^{203}Hg] in each sample was determined by counting in a Wallac Wizard 3 automatic gamma counter (Perkin Elmer, Boston, MA) and the content of Hg^{2+} in each sample was estimated using standard computational methods.

2.5. Histological analyses

Kidneys were fixed in fixative described above for 48 h at 4 °C. Following fixation, kidneys were washed twice with normal saline and placed in 70 % ethanol. Tissues were processed in a Tissue-Tek VIP processor using the following sequence: 95 % ethanol for 30 min (twice); 100 % ethanol for 30 min (twice); 100 % xylene (twice). Tissue was subsequently embedded in POLY/Fin paraffin (Fisher) and 5 μm sections were cut using a Leitz 1512 microtome and were mounted on glass slides. Sections were stained with hematoxylin and eosin (H & E) and were viewed using an Olympus IX70 microscope. Images were captured with a Jenoptix Progress C12 digital camera.

2.6. Quantitative PCR

RNA was isolated from frozen sections of rat kidney using TRIzol Reagent (Invitrogen) according to the manufacturer's protocol. Reverse transcription of 1 μg of RNA was carried out using reverse transcriptase and random hexamers (Life Technologies). Quantitative PCR analyses of metallothionein 1a (MT1a) and kidney injury molecule-1 (Kim-1) expression were performed using an ABI Prism 7300 sequence detection system and commercially available gene expression assays (MT1a; Rn00821759_g1; Kim-1; Rn00597703_m1, Life Technologies). Glyceraldehyde-3-phosphate dehydrogenase (Gapdh) (Hs02786624_g1; Life Technologies) was used as a reference gene.

2.7. Isolated proximal tubule experiments

Rabbit kidneys are well suited for the dissection of individual nephron segments because they contain very little connective tissue,

unlike mice and rats, which require digestion with collagenase. Rabbits were anesthetized with an intramuscular injection of ketamine (70 mg kg^{-1}) and xylazine (30 mg kg^{-1}). A two-inch incision was made in the right flank and the renal artery and vein were ligated using 2–0 nylon suture. The right kidney was removed and placed in ice-cold sucrose buffer (14 mM NaH_2PO_4, 56 mM Na_2HPO_4, 125 mM sucrose, pH 7.4). The incision was closed with 4–0 silk suture. The renal capsule was removed, and the kidney was sectioned transversely to yield slices with a thickness of approximately 1–2 mm as described previously (Zalups and Barfuss, 1996a, b).

S2 segments of proximal tubules (approximately 1 mm in length) were dissected from the inner and middle regions of cortical medullary rays. For perfused tubule experiments (Zalups, 1996a), isolated tubules were transferred to an acrylic perfusion chamber containing artificial perfusion medium (APM; 148 mM NaCl, 5 mM KCl, 1.3 mM $CaCl_2$, 2.0 mM NaH_2PO_4, 0.5 mM L-glutamine, 1.0 mM D-glucose, pH 7.4) on the stage of a Jena Sedival inverted microscope. One end of the tubule was gently suctioned into a holding pipette. The opposite end was gently suctioned into a collection pipet. A perfusion pipet containing perfusate was inserted into the lumen of the tubule at the holding end. The perfusate for the proximal tubular experiments contained 10 μM [^{203}Hg], 22.5 μM metallothionein 1A (MT1A; MyBioSource) or 22.5 μM glutathione (GSH), and 5 μM [^{3}H]-L-glucose as a volume marker. [^{203}Hg] and [^{3}H]-L glucose were dried down as described previously and resuspended with APM (Zalups, 1996b). MT1A or GSH was added to the solution to yield a final volume of 22.5 μM. Hg-MT or GSH-Hg-GSH complexes were formed by allowing the solution to sit at room temperature for a minimum of 10 min. Tubules were perfused at a rate of 10 nL min^{-1} at 37 °C. The timed collectate samples were measured and placed in individual scintillation vials to determine the transport rate of Hg. Three sequential collections were made, and the experiment was repeated three additional times (n = 9). Samples were counted using a Beckman LS6500 scintillation counter.

For experiments using non-perfused S2 tubules, three proximal tubules (1 mm each) were dissected from the cortical medullary rays of a section of rabbit kidney. Tubules were incubated for 1 min in 10 μL of [^{203}Hg]-MT solution in a terasaki plate (Greiner). For pitstop experiments, tubules were incubated in 30 μM pitstop in APM for 30 min, following which tubules were incubated in [^{203}Hg]-MT for 1 min. Following the incubation with MT-Hg, tubules were quickly rinsed (less than 1 sec) in APM containing 1 mM 2,3-dimercapto-1-propanesulfonic acid (DMPS) to remove Hg bound to the outside of the tubule. Tubules were then placed in 10 μL 3 % (w/v) trichloroacetic acid (TCA), which precipitates large intracellular proteins and releases cytosolic contents. The DMPS solution, TCA solution and the tubule were transferred to separate scintillation vials containing OptiFluor scintillation liquid (PerkinElmer). Experiments were repeated twice, using a total of 9 tubules. Samples were counted in a Beckman scintillation counter.

2.8. Statistical analyses

Data for each rat experiment were analyzed first with the Kolmogorov-Smirnov test for normality and then with Leven's test for homogeneity of variances. Data were then analyzed using a two-way analysis of variance (ANOVA) or a *t*-test to assess differences among the means. When statistically significant *F*-values were obtained with ANOVA, the data were analyzed using Tukey's *post hoc* multiple comparison test. A p-value of ≤ 0.05 was considered statistically significant. Each group of animals contained four rats.

3.0. Results

3.1. Expression of MT

The expression of mRNA encoding MT1a was assessed in kidney and liver from male and female rats injected with saline or Zn (Fig. 1).

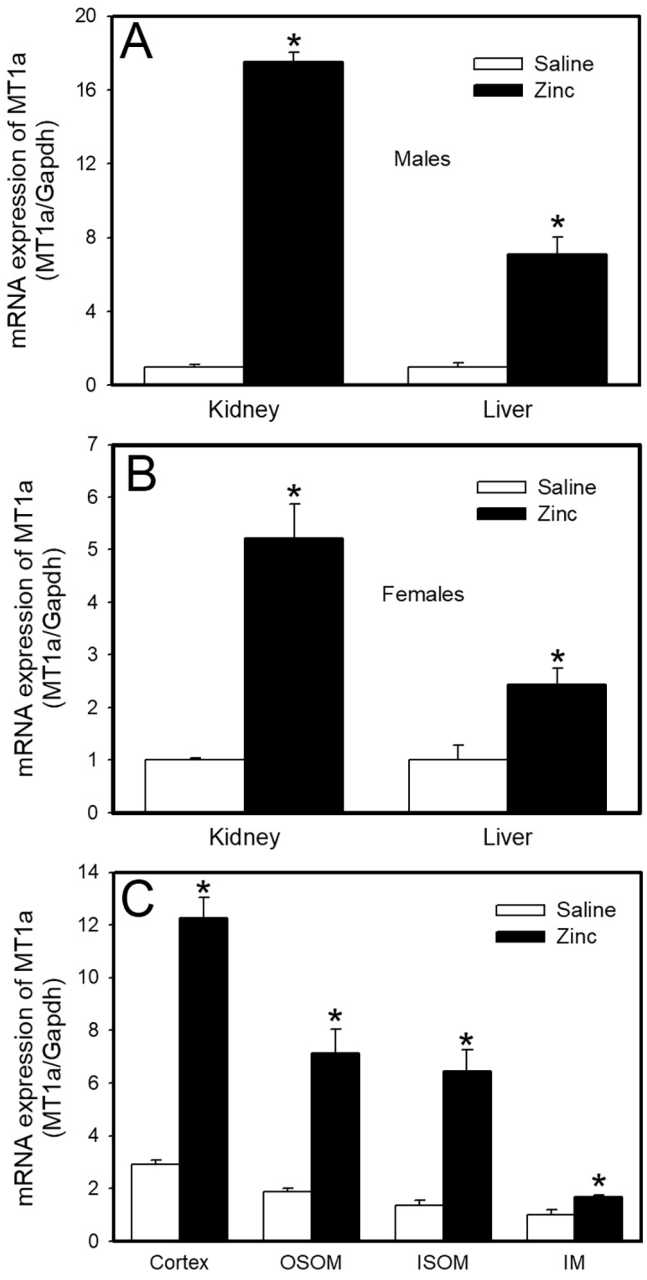

Fig. 1. Expression of Metallothionein. Quantitative PCR (qPCR) analysis of metallothionein 1a (MT1a) was carried out using mRNA extracted from kidney and liver from male (A) and female (B) rats exposed to saline or Zn (25 mg/kg). Also, qPCR was used to analyze expression of MT1a in the renal cortex, outer stripe of outer medulla (OSOM), inner stripe of outer medulla (ISOM), and inner medulla (C). Gapdh was used as a reference gene. n = 6. *, significantly different ($p < 0.5$) from the mean of the corresponding group exposed to saline.

Expression was significantly greater in kidney and liver of Zn-injected rats compared with saline-injected controls. This was true in both male (A) and female (B) rats. The expression of mRNA encoding MT1a was measured in each renal zone (C). Data shown are representative of expression in male and female rats. The cortex exhibited the greatest expression of MT1a, followed by the outer stripe of the outer medulla (OSOM), inner stripe of the outer medulla, and the inner medulla. Injection with Zn significantly enhanced the expression in each zone. It is recognized that other isoforms of MT1 and also, MT2, are present in the kidney. Their distribution and roles are similar to that of MT1a; thus, we consider the mRNA expression of MT1a to be representative of other MT isoforms.

3.2. Renal accumulation of Hg

The amount of Hg in the total renal mass of males (A) and females (B) is shown in Fig. 2. In male rats, pre-injection of Zn increased renal accumulation of Hg in rats exposed to 1.5 and 2.25 μmol $HgCl_2$, but not in rats exposed to 0.5 μmol $HgCl_2$. In contrast, when female rats were injected with Zn, the renal accumulation of Hg increased significantly in each group of rats. The Hg accumulation in the total renal mass of males was similar to that of females.

The amount of Hg in the cortex (Fig. 3) of male (A) and female (B) rats was measured. When male rats were injected with Zn, the accumulation of Hg in the cortex increased significantly in rats exposed to 1.5 and 2.25 μmol kg^{-1} $HgCl_2$ compared with saline-injected controls. Interestingly, injection with Zn did not alter the accumulation of Hg in rats exposed to 0.5 μmol kg^{-1} $HgCl_2$. In female rats (B), injection with Zn increased the cortical accumulation of Hg in each group of rats (0.5, 1.5, 2.25 μmol $HgCl_2$) compared with controls. There was minimal accumulation of Hg in the inner stripe of the outer medulla and the inner medulla (data not shown).

Fig. 4 shows the pattern of accumulation of Hg in the OSOM of male (A) and female (B) rats, which was different than that measured in the cortex. In male rats, injection with Zn did not significantly alter the accumulation of Hg in any group of rats. In female rats, there was no significant difference in Hg accumulation between control and Zn-injected rats injected with 0.5 or 1.5 μmol $HgCl_2$, but statistically significant differences were observed when females were injected with 2.25 μmol $HgCl_2$.

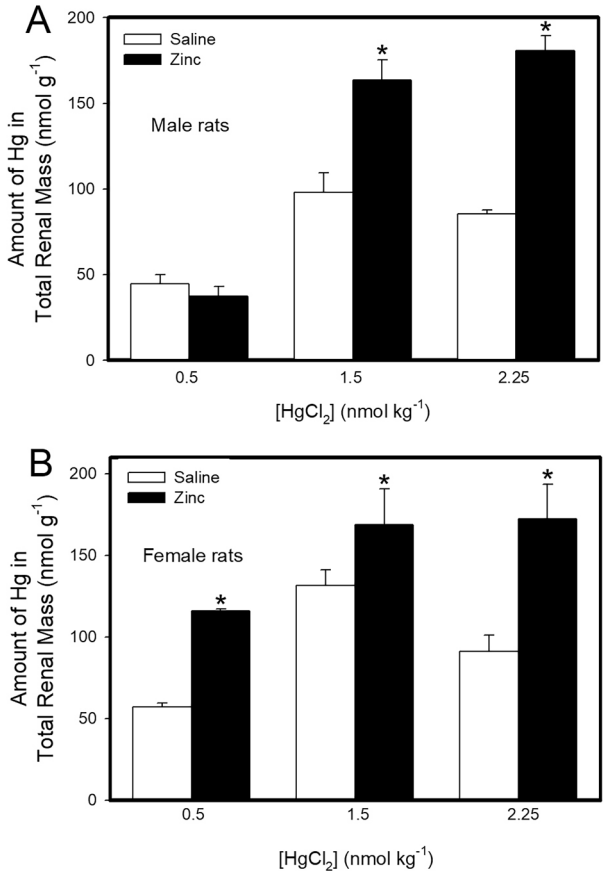

Fig. 2. Amount of Hg in Total Renal Mass. The amount of Hg in the total renal mass was measured in male (A) and female (B) rats injected with saline or Zn (25 mg/kg) and exposed 24 h later to $HgCl_2$. Rats were euthanized 24 h after injection with $HgCl_2$. n = 4. *, significantly different ($p < 0.5$) from the mean of the corresponding group exposed to saline.

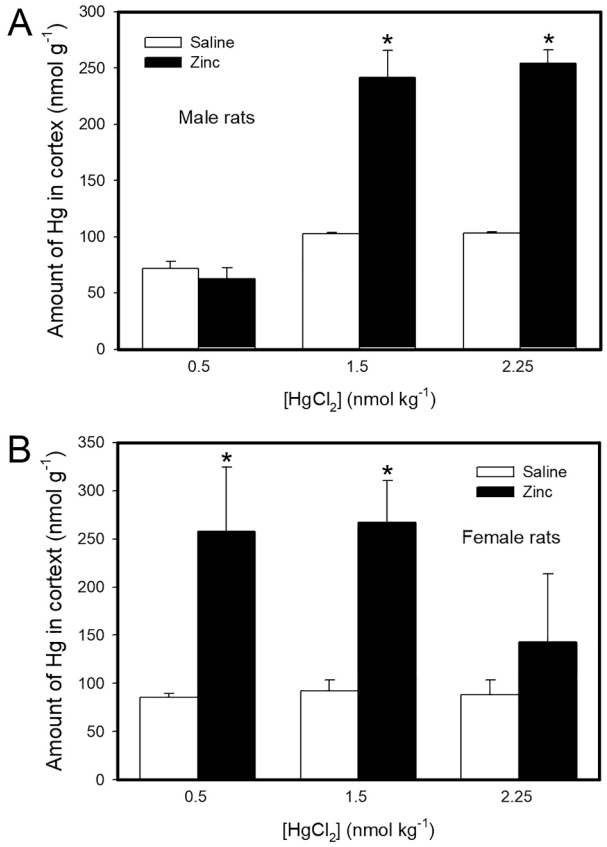

Fig. 3. Amount of Hg in Renal Cortex. The amount of Hg in the renal cortex was measured in male (A) and female (B) rats injected with saline or Zn (25 mg/kg) and exposed 24 h later to $HgCl_2$. Rats were euthanized 24 h after injection with $HgCl_2$. n = 4. *, significantly different ($p < 0.5$) from the mean of the corresponding group exposed to saline.

3.3. Urinary excretion of Hg

Urinary excretion (Fig. 5) was measured in each group of rats. In males (A), the urinary excretion of Hg was significantly lower in rats injected with Zn than in corresponding rats injected with saline. This was true for all three concentrations of $HgCl_2$ injected. In female rats (B), there was no significant difference in Hg excretion between Zn- and saline-injected rats following exposure to 0.5 and 2.25 μmol kg^{-1} $HgCl_2$, but in female rats injected with 1.5 μmol kg^{-1} $HgCl_2$, the urinary excretion of Hg was significantly less in the Zn group than in the saline group.

3.4. Hepatic burden of Hg

The hepatic burden of Hg is shown in Fig. 6. When male rats (A) were injected with Zn and exposed to 0.5 or 2.25 μmol $HgCl_2$, the accumulation of Hg was not significantly different between Zn-injected rats and saline-injected rats. However, when rats were exposed to 1.5 μmol $HgCl_2$, the hepatic accumulation of Hg was greater in Zn-injected rats than in their saline-injected counterparts. Interestingly, when female rats (B) were injected with Zn and exposed to 0.5 or 1.5 μmol kg^{-1} $HgCl_2$, the hepatic burden of Hg was significantly greater in Zn-injected rats than in corresponding saline controls. In contrast, when females were injected with 2.25 μmol kg^{-1} $HgCl_2$, the hepatic accumulation of Hg was not significantly different between Zn-injected and saline-injected rats.

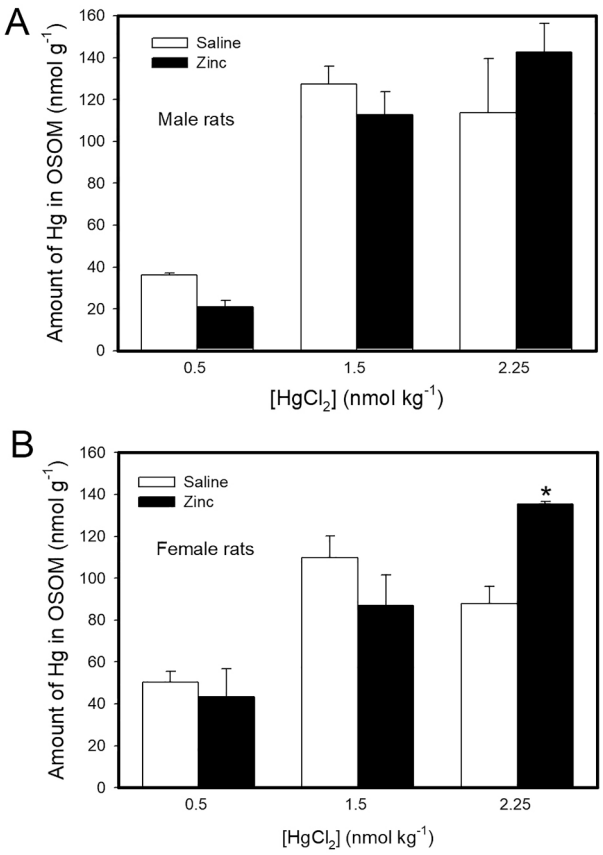

Fig. 4. Amount of Hg in Outer Stripe of the Outer Medulla. The amount of Hg in the outer stripe of the outer medulla (OSOM) was measured in male (A) and female (B) rats injected with saline or Zn (25 mg/kg) and exposed 24 h later to $HgCl_2$. Rats were euthanized 24 h after injection with $HgCl_2$. n = 4. *, significantly different ($p < 0.5$) from the mean of the corresponding group exposed to saline.

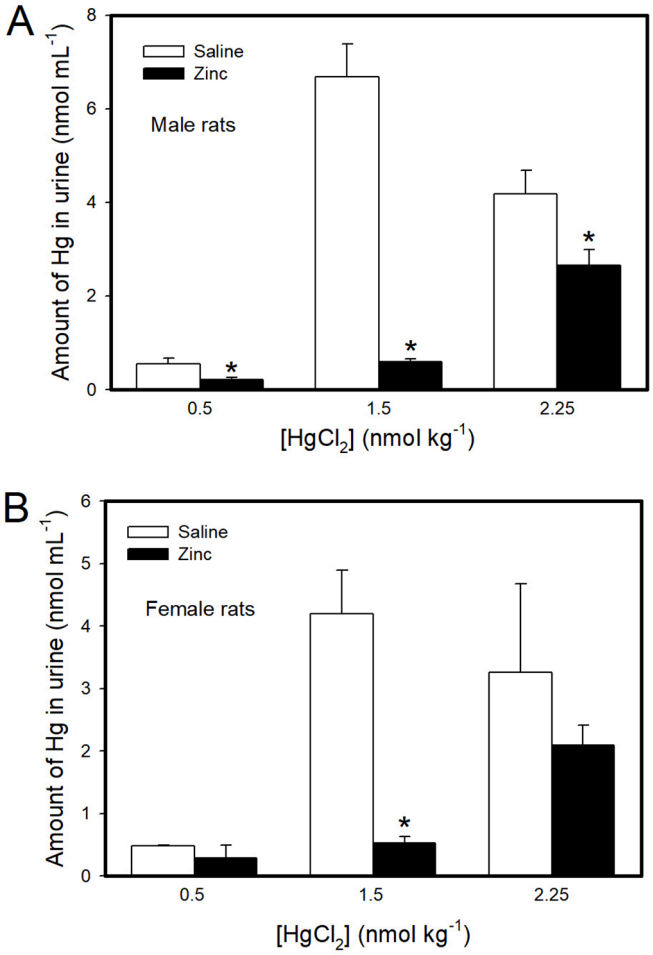

Fig. 5. Amount of Hg in Urine. The amount of Hg in urine was measured in male (A) and female (B) rats injected with saline or Zn (25 mg/kg) and exposed 24 h later to $HgCl_2$. Rats were euthanized 24 h after injection with $HgCl_2$. n = 4. *, significantly different ($p < 0.5$) from the mean of the corresponding group exposed to saline.

3.5. Hematologic burden of Hg

Fig. 7 shows the content of Hg in blood from male (A) and female (B) rats. In both sexes, there was no significant difference in the amount of Hg in blood of Zn-injected and saline-injected rats exposed to 0.5 or 1.5 μmol kg^{-1} $HgCl_2$. In contrast, in male and female rats exposed to 2.25 μmol kg^{-1} $HgCl_2$, the amount of Hg in blood of saline-injected rats was significantly greater than that of Zn-injected rats.

3.6. Fecal excretion of Hg

Fecal excretion of Hg (Fig. 8) was measured in male (A) and female (B) rats. In male rats, fecal excretion of Hg was significantly greater in saline-injected rats than in Zn-injected rats following exposure to 1.5 or 2.25 μmol $HgCl_2$. In females, the fecal content of Hg was significantly greater in saline-injected rats than in Zn-injected rats at every concentration of $HgCl_2$.

3.7. Analysis of Hg-induced nephrotoxicity

Histological analyses were performed on kidneys (Fig. 9) from each group of rats. There were no observable differences between males and females; thus, the images shown are considered to be representative of both sexes. The 0.5 μmol kg^{-1} dose of $HgCl_2$ is considered to be a non-nephrotoxic dose and as expected, the cortex and OSOM of rats exposed to this dose of Hg appeared normal. When saline-injected rats were exposed to a moderately nephrotoxic dose of $HgCl_2$ (1.5 μmol kg^{-1}), a few proximal tubules (arrows) within the cortex appeared swollen but not necrotic. In the OSOM of these rats, necrosis (*) was evident and widespread among proximal tubules. In contrast, kidneys of corresponding Zn-injected rats showed minimal nephrotoxic change. In the OSOM of kidneys from rats exposed to Zn and injected with 1.5 μmol $HgCl_2$, a few proximal tubules (arrows) appeared swollen but necrosis was not visible. The severity of Hg-induced renal injury increased substantially when rats were injected with 2.25 μmol kg^{-1} $HgCl_2$. In rats injected with saline followed by exposure to 2.25 μmol $HgCl_2$, significant necrosis (arrows) was observed throughout the cortex and OSOM. In addition, many tubules appeared to be filled with proteinaceous casts (arrowheads). In corresponding rats injected with Zn, there was minimal change in the cortex and significantly less necrosis (arrows) in the OSOM.

Quantitative PCR was used to assess the expression of mRNA encoding Kim-1 in kidneys from each group of rats (Fig. 10). The expression of Kim-1 in male (A) and female rats (B) injected with '0.5 μmol $HgCl_2$ was minimal and was not significantly altered by pre-injection with Zn. In contrast, Kim-1 expression increased significantly in rats pre-injected with saline followed by exposure to 1.5 or 2.25 μmol $HgCl_2$ (compared with rats injected with 0.5 μmol $HgCl_2$). In corresponding rats pre-injected with Zn, the expression of Kim-1 also increased significantly, but the magnitude of the increase was significantly less than that observed in corresponding saline-injected rats. This pattern of expression was observed in both, male and female rats.

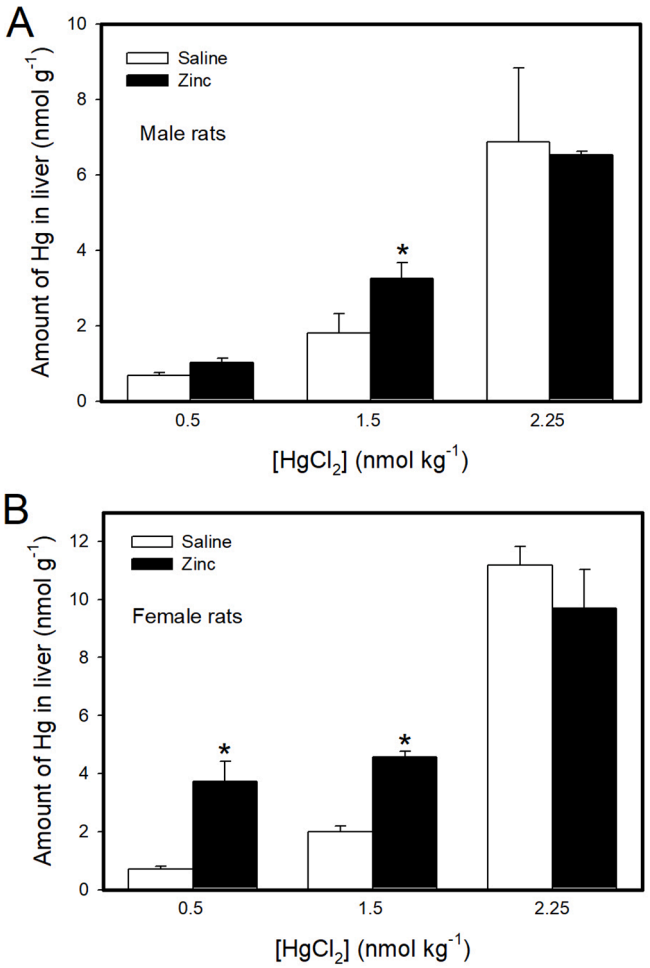

Fig. 6. Amount of Hg in Liver. The amount of hg in liver was measured in male (A) and female (B) rats injected with saline or Zn (25 mg/kg) and exposed 24 h later to $HgCl_2$. Rats were euthanized 24 h after injection with $HgCl_2$. n = 4. *, significantly different ($p < 0.5$) from the mean of the corresponding group exposed to saline.

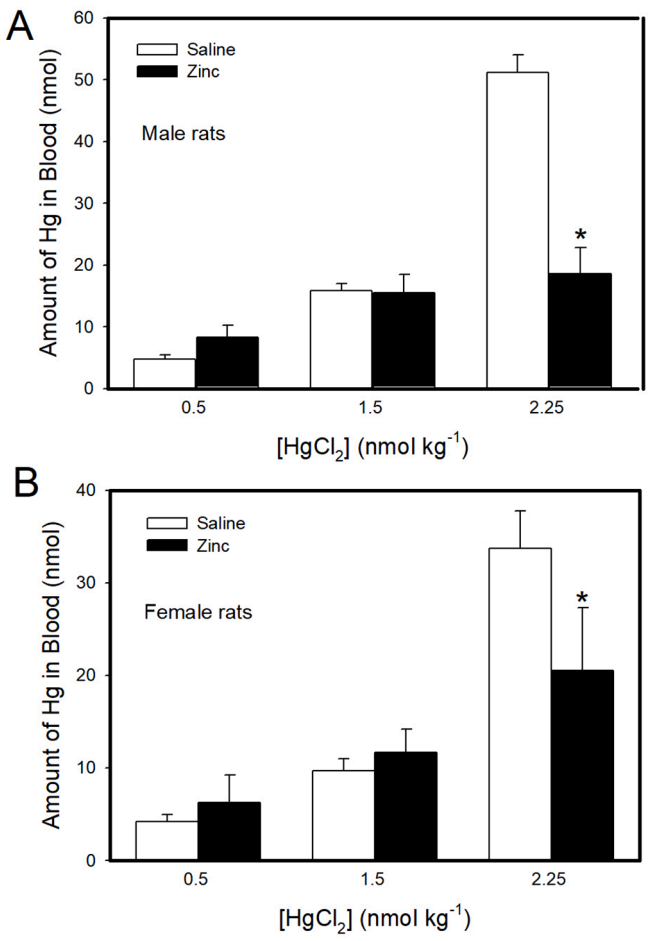

Fig. 7. Amount of Hg in Blood. The amount of Hg in blood was measured in male (A) and female (B) rats injected with saline or Zn (25 mg/kg) and exposed 24 h later to $HgCl_2$. Rats were euthanized 24 h after injection with $HgCl_2$. n = 4. *, significantly different ($p < 0.5$) from the mean of the corresponding group exposed to saline.

3.8. *Proximal tubular transport of Hg-MT*

The luminal disappearance of Hg-MT complexes (disappearance flux, J_D; Fig. 11A) and the cellular accumulation (Fig. 11B) was measured in isolated S2 segments of proximal tubules. Luminal disappearance is an indication of apical uptake. The uptake of Hg-MT was significantly greater than that of GSH-Hg-GSH, which is thought to be the primary form of Hg presented to the luminal membrane of proximal tubules under normal conditions. The cellular accumulation of Hg following luminal perfusion of Hg-MT or GSH-Hg-GSH was similar. The basolateral uptake of Hg-MT was measured in non-perfused S2 segments of proximal tubules (Fig. 11C). Hg-MT complexes were taken up readily from the basolateral membrane and this uptake was significantly reduced by pitstop, an inhibitor of endocytosis.

4.0. *Discussion*

Many studies have examined the effects of MT on the disposition and toxicity of cadmium in various organs (Chan et al., 1992; Nordberg and Nordberg, 2022; Park et al., 2001), but there are still major knowledge gaps regarding how MT expression affects the handling and disposition of Hg. *In vivo and vitro* studies have shown that exposure to Hg results in an upregulation of MT expression (Agarwal et al., 2010; Agrawal et al., 2014; Oliveira et al., 2020; Zalups and Koropatnick, 2000). Moreover, increased expression of MT has been shown to prevent Hg-induced inhibition of δ-aminolevulinic acid dehydratase and also provided some protection against Hg-induced reductions in GFR in *in vivo* models (Mesquita et al., 2016; Oliveira et al., 2020). Studies using *in vitro* models have also shown that upregulation of MT protects against many Hg-induced cellular alterations, including reduced cell viability, DNA damage, and increased reactive oxygen species (Hossain et al., 2021). Despite these studies, there is little information regarding the effects of MT upregulation on the uptake and disposition of Hg in target cells and organs. Therefore, the current study was designed to examine the effects of MT overexpression on the in vivo disposition and toxicity of Hg in target organs of male and female rats. Furthermore, the current study also examined the transport of Hg-MT complexes at the luminal and basolateral membranes of proximal tubular cells.

The current findings demonstrated that overexpression of MT enhances the total renal burden of Hg. More specifically, we observed a significant increase in the cortical accumulation of Hg when MT was overexpressed. This was different from that in the OSOM where the accumulation of Hg was not altered by overexpression of MT. One possible reason for the observed difference in accumulation may be related to the pattern of MT expression in the renal zones and the normal handling of mercuric ions. Previous studies in mice and rats have shown that MT is localized primarily in proximal tubules of the cortex (Fujishiro et al., 2022; Nishimura et al., 1989; Sabolic et al., 2018). Indeed, our quantitative PCR data show that mRNA expression of MT is

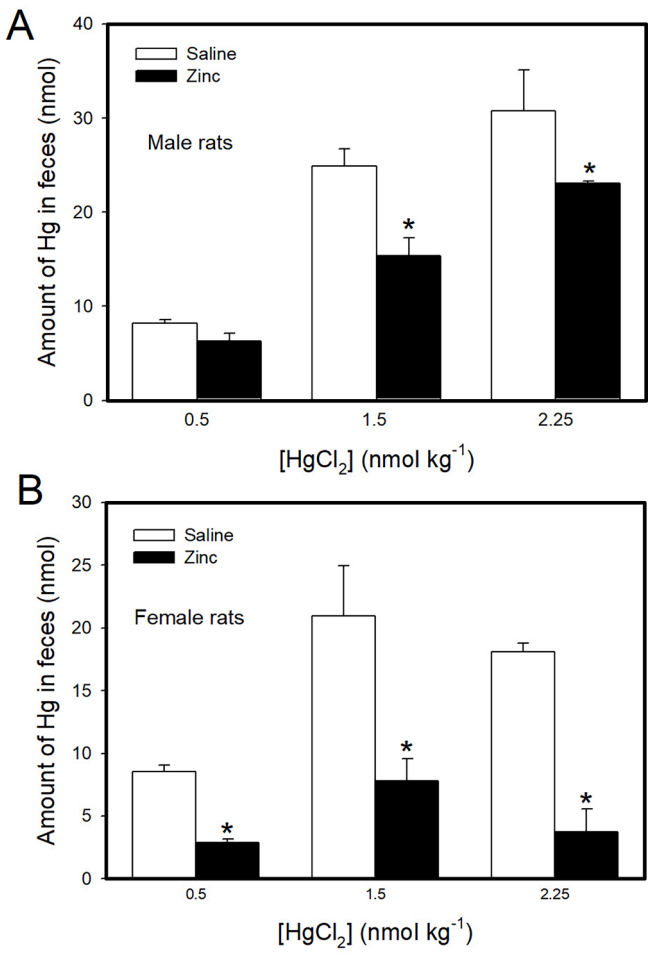

Fig. 8. Amount of Hg in Feces. The amount of Hg in feces was measured in male (A) and female (B) rats injected with saline or Zn (25 mg/kg) and exposed 24 h later to $HgCl_2$. Rats were euthanized 24 h after injection with $HgCl_2$. n = 4. *, significantly different ($p < 0.5$) from the mean of the corresponding group exposed to saline.

greater in the cortex than in other zones of the kidney. After mercuric species (e.g., Cys-Hg-Cys; GSH-Hg-GSH, etc.) are taken up by proximal tubular cells, the enhanced expression of MT would likely lead to cellular retention of Hg. MT has a very high affinity for Hg; thus, mercuric ions that are not already bound to MT may bind to MT within the cytoplasm to form large Hg-MT complexes that may be retained in the cell. This will be particularly true in segments of proximal tubules that have higher levels of MT, i.e., cortical proximal tubules. MT is capable of binding 6–11 molecules of Hg (He et al., 2021); thus, it is logical that cells and tissues with higher levels of MT will accumulate more Hg. Another factor that may contribute to this pattern of accumulation is the axial heterogeneity of transport mechanisms along the proximal tubule. Receptor-mediated endocytosis occurs largely in S1 proximal tubules (Carney, 2019), which are present exclusively in the cortex. As discussed below, we propose that receptor-mediated endocytosis plays a role in the cellular uptake of Hg-MT complexes.

Although renal accumulation of Hg is rapid, it appears as though cellular export could be somewhat slow. We have shown that certain Hg complexes (e.g., GSH-Hg-GSH) can be exported from the apical membrane of proximal tubular cells by the multidrug resistance-associated protein 2 (Mrp2) (Bridges et al., 2008a, b) and the breast cancer resistance protein (Bcrp) (Bridges et al., 2015). It is not likely that these carriers are able to mediate the export of Hg-MT complexes due to the large size of the complexes. Therefore, export of these complexes may be dependent upon degradation of MT or thiol exchange whereby Hg is released from MT to bind to a smaller thiol-containing molecule. The half-life of MT has been estimated to be 4–5 days, yet the half-life of the Zn-MT complex (and possibly Hg-MT) appears to be around 20——30 h (Cherian and Goyer, 1978; Piletz et al., 1983). As MT proteins are degraded, any associated Hg is likely released into the cytoplasm where it forms conjugates with intracellular thiols such as GSH or cysteine. These conjugates can then be exported into the tubular lumen via apical transport mechanisms. Experiments with endpoints longer than those in the current study may be able to capture this process.

To our knowledge, there are no published studies that provide direct evidence that Hg-MT complexes are taken up by proximal tubular cells. Since MT levels in blood increase after injection with Zn, it is likely that Hg-MT complexes are formed in blood and subsequently delivered to proximal tubules. Therefore, it is important to determine if and how these complexes are taken up by proximal tubular cells. The current study utilized isolated perfused and non-perfused proximal tubules to assess apical and basolateral uptake of Hg-MT complexes. The data from these experiments indicate that Hg-MT complexes are taken up at both, the luminal and basolateral membranes of proximal tubules. The disappearance flux (J_D) measures the rate by which a substrate leaves the lumen and is taken up by tubular cells. The J_D of Hg-MT was significantly greater than that of GSH-Hg-GSH, suggesting that its transport into cells is more rapid than that of GSH-Hg-GSH. Interestingly, the cellular accumulation of Hg-MT was similar to that of GSH-Hg-GSH suggesting that that although Hg-MT is taken up faster, the mechanisms responsible for its apical uptake may become saturated more quickly and consequently limit cellular accumulation of Hg-MT complexes. The mechanism(s) by which these complexes are taken up remain to be identified; however, it appears that some form of endocytosis may be involved in this process. Pitstop, a well-known inhibitor of endocytosis (Dutta et al., 2012), reduced the basolateral accumulation of Hg-MT complexes by approximately 50 %. Assessing the effects of pitstop on the apical uptake of Hg-MT is not technically feasible using the isolated perfused tubule technique. Interestingly, published findings from studies in cultured proximal tubular cells suggested that apical uptake of MT-cadmium complexes is dependent upon megalin, a receptor involved in endocytosis (Wolff et al., 2006). Considering our current data and that of other labs, we suggest that endocytosis may mediate at least part of Hg-MT uptake in proximal tubular cells. Other mechanisms are likely involved in this uptake and thus, additional studies are necessary to fully elucidate this process.

The current data show that increased expression of MT protects against Hg-induced renal injury. There were no obvious differences in the histopathology between corresponding groups of male and female rats. The 0.5 μmol dose represents a non-nephrotoxic dose of Hg; no injury was observed in these groups. In contrast, when animals were exposed to 1.5 or 2.5 μmol Hg, obvious pathological changes in the renal cortex and OSOM were observed. Kidneys of rats injected with 1.5 μmol Hg displayed tubular swelling in the cortex and pyknosis, cellular degeneration, and necrosis in the OSOM. Treatment of rats with Zn was largely protective against this dose of Hg. In Zn-injected rats, the cortex appeared normal and although the OSOM exhibited tubular swelling, there was no evidence of cellular necrosis and death. When rats were injected with 2.5 μmol Hg, renal injury was more extensive and severe than in rats injected with the lower dose. At this dose, significant cellular injury and necrosis was observed in both the cortex and the OSOM. Injection with Zn protected cortical tubules from injury and lessened the severity of necrosis in the OSOM. This pattern of injury may be due, in part, to the axial heterogeneity of MT expression along the nephron, with higher expression in cortical segments than in those located in the OSOM. The mRNA expression of a well-known biomarker of renal injury, Kim-1, further confirmed that injection with Zn significantly reduced Hg-induced renal injury.

In the liver, MT expression was enhanced by exposure to Zn. This enhanced the hepatic accumulation of Hg in animals exposed to lower doses of Hg (0.5, 1.5 μmol). Our previous work suggests that Hg-albumin

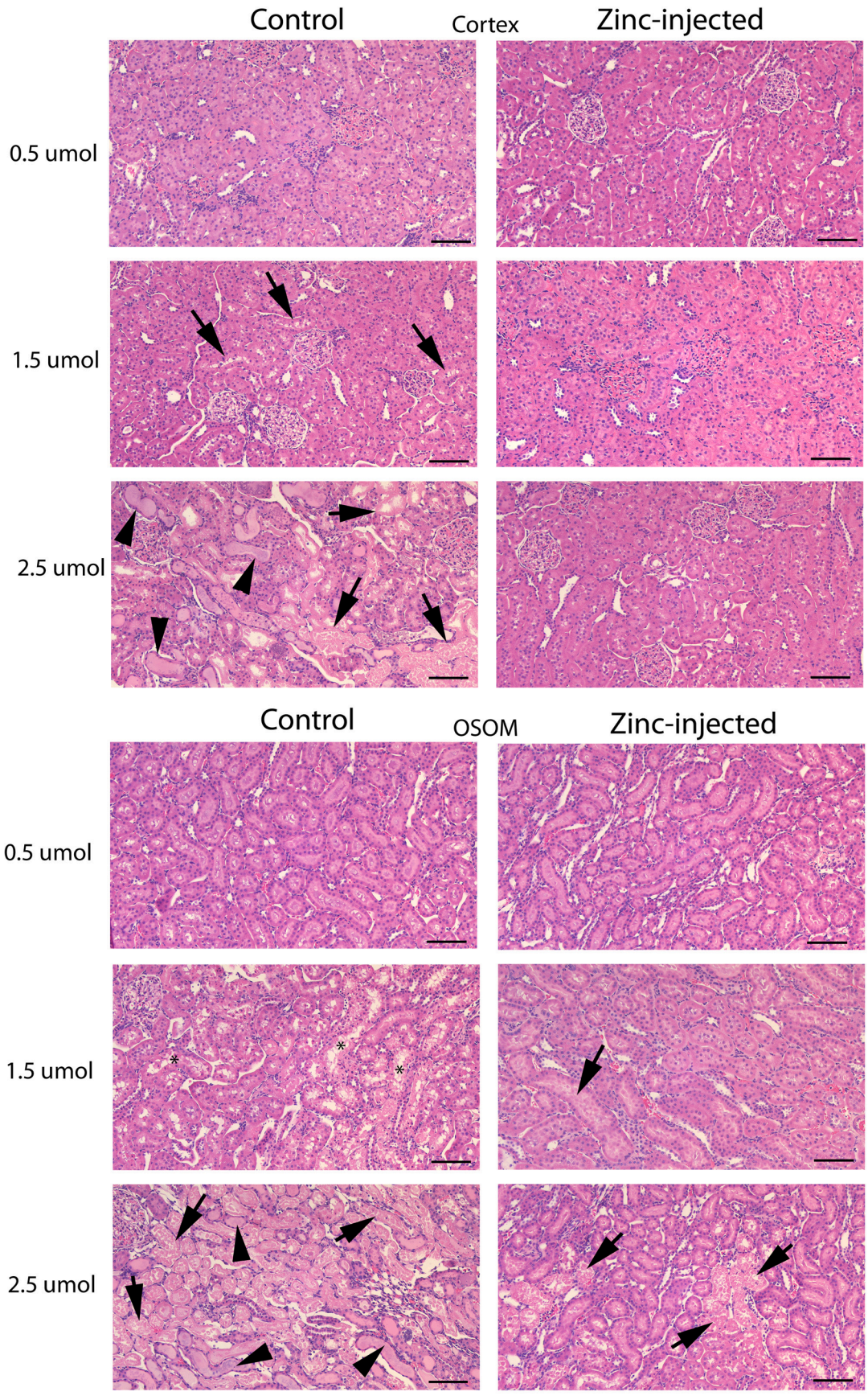

(caption on next page)

Fig. 9. Histological Analysis of Renal Injury. Rats were exposed to saline (Control) or Zn (25 mg/kg) followed by injection with $HgCl_2$ (0.5, 1.5, or 2.25 μmol kg^{-1} 2 mL^{-1}) 24 h later. Rats were euthanized 24 h after injection with $HgCl_2$ and kidneys were fixed for histological analyses. Sections were stained with hematoxylin and eosin. Little injury was observed in the cortex or outer stripe of the outer medulla (OSOM) of rats exposed to 0.5 μmol $HgCl_2$. When rats were exposed to 1.5 μmol $HgCl_2$, a few swollen tubules (asterisk) were identified in the cortex while obvious necrosis (arrows) was observed in the OSOM of rats exposed to saline. In corresponding Zn-injected rats, the injury was noticeably less severe. Only a few swollen tubules were present and no necrosis was observed. When rats were exposed to 2.25 μmol $HgCl_2$, numerous tubules had evidence of proteinaceous casts (arrowheads) and necrosis (arrows) in the cortex and OSOM. Treatment with Zn reduced the severity of this injury so that there were fewer necrotic tubules (arrows).

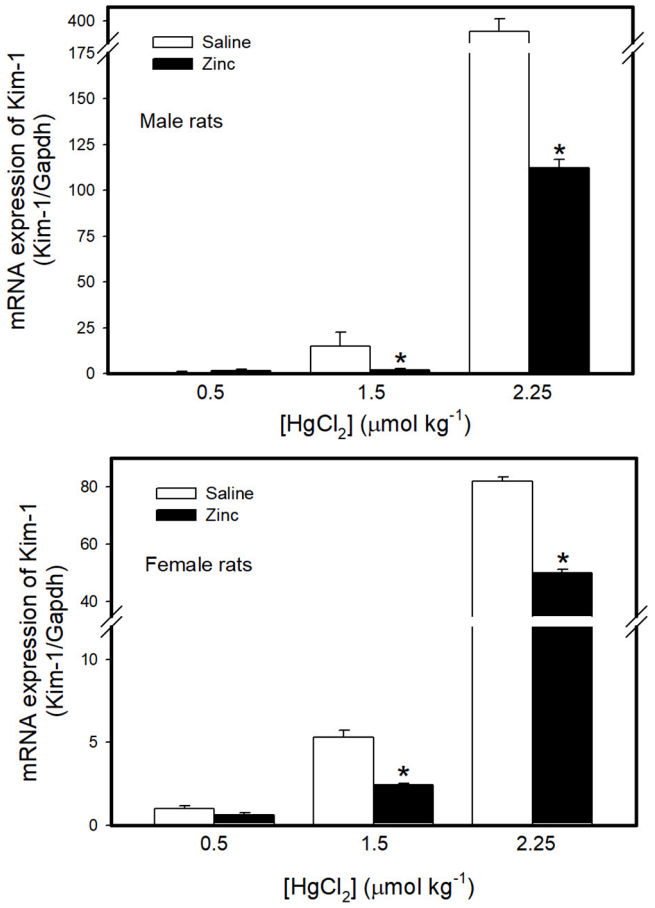

Fig. 10. Expression of Kidney Injury Molecule-1. The expression of kidney injury molecule-1 (Kim-1) was assessed using mRNA isolated from kidneys of rats treated with saline or Zn (25 mg/kg) followed 24 h later with injection of $HgCl_2$ (0.5, 1.5, or 2.25 μmol kg^{-1}). Rats were euthanized 24 h after injection with $HgCl_2$. n = 6. *, significantly different ($p < 0.5$) from the mean of the corresponding group exposed to saline.

complexes are taken up into hepatocytes by endocytosis, following which, they are conjugated to a different ligand such as GSH to facilitate excretion. However, when the expression of MT is enhanced, intracellular Hg may bind to MT and accumulate within the hepatocyte. Overexpression of MT did not affect hepatic accumulation of Hg at the highest dose of Hg (2.25 μmol), likely because at this concentration, the mechanisms involved in transporting Hg into hepatocytes are saturated. Fecal excretion of Hg was reduced in animals overexpressing MT, supporting the idea that Hg binds to MT within hepatocytes and slows the ability of hepatocytes to export it into blood or bile. Hg may be slowly exported as it undergoes ligand exchange and binds to a ligand that creates a mercuric species that is more readily transportable than Hg-MT.

The amount of Hg in blood of animals exposed to 0.5 and 1.5 μmol Hg was not altered by overexpression of MT. One might expect the blood levels of Hg in Zn-injected rats to be lower than those of control rats due to sequestration of Hg in organs. This finding may be explained by the low urinary excretion of Hg in Zn-injected rats. Cellular accumulation of Hg due to overexpression of MT is likely due to an inability to export Hg for excretion rather than enhanced uptake of Hg-MT from the blood. Interestingly, when rats were exposed to 2.5 μmol Hg, the amount of Hg in blood was significantly less in Zn-injected animals than in saline-injected animals. The urinary excretion of Hg also increased in Zn-injected animals exposed to 2.5 μmol Hg, which may account for the differences in blood levels of Hg.

Previous studies from our lab have shown that the distribution of Hg varies between sexes (Pittman et al., 2020); therefore, the currently study was performed in males and females. In the present study, we observed differences in the pattern of Hg accumulation in the renal cortex and OSOM between the sexes. These differences may be due to different patterns of MT distribution in males and females, which has been shown in previous studies (Ljubojevic et al., 2019; Zhang et al., 2012). Although differences in the pattern of Hg accumulation were observed between males and females, we did not observe differences in histopathological change between sexes, suggesting that both sexes are equally susceptible to Hg-induced nephrotoxicity.

In summary, the current study is the first to demonstrate that Hg-MT complexes are taken up at the luminal and basolateral membranes of proximal tubular cells. In addition, our data suggest that endocytosis may be one mechanism by which Hg-MT complexes are taken up into proximal tubular cells. Moreover, the current data show that although overexpression of MT enhances the renal accumulation of Hg, it also protects against Hg-induced nephrotoxicity. This is likely due to the binding of Hg to MT and the formation of a stable complex that has low oxidative activity. Therefore, supplementation with Zn in individuals at risk of occupational, dietary, and environmental exposure to Hg may be a viable strategy for reducing the risk of Hg intoxication.

Our current findings suggest that overexpression of MT alters the corporal disposition of Hg. Under normal conditions, a large fraction of Hg in blood appears to be bound to albumin, forming Hg-albumin complexes, which are taken up subsequently into hepatocytes and processed to form GSH-conjugates of Hg. These GSH-Hg conjugates are then exported and delivered to the kidney for filtration and eventual excretion. (Barfuss et al., 2022). After glomerular filtration, GSH-Hg conjugates are taken up at the apical and basolateral plasma membranes of proximal tubular cells and mercuric ions accumulate within the cells. We propose that when expression of MT is upregulated and more MT is present in blood, some of the mercuric ions that would normally be bound to albumin or GSH will bind to MT. Hg-MT conjugates will then be delivered to liver and kidney. Our data suggest that renal uptake of these conjugates occurs via endocytosis. In addition to Hg-MT conjugates, Hg-GSH conjugates will also be delivered to hepatocytes and proximal tubular cells. As these conjugates are taken up into target cells, mercuric ions will bind to MT in these cells and Hg accumulation as it binds mercuric ions.

CRediT authorship contribution statement

Aditi Dave: Investigation, Writing – original draft, Writing – review & editing. **Lucy Joshee:** Investigation, Writing – review & editing. **Delon W. Barfuss:** Conceptualization, Investigation, Methodology, Writing – review & editing. **Ryan Brownlee:** Investigation, Writing – review & editing. **Roha Surani:** Investigation, Writing – review & editing. **Sahar Anis Ali:** Investigation, Writing – review & editing. **Earl G. Ford IV:** Investigation, Writing – review & editing. **Elizabeth G.**

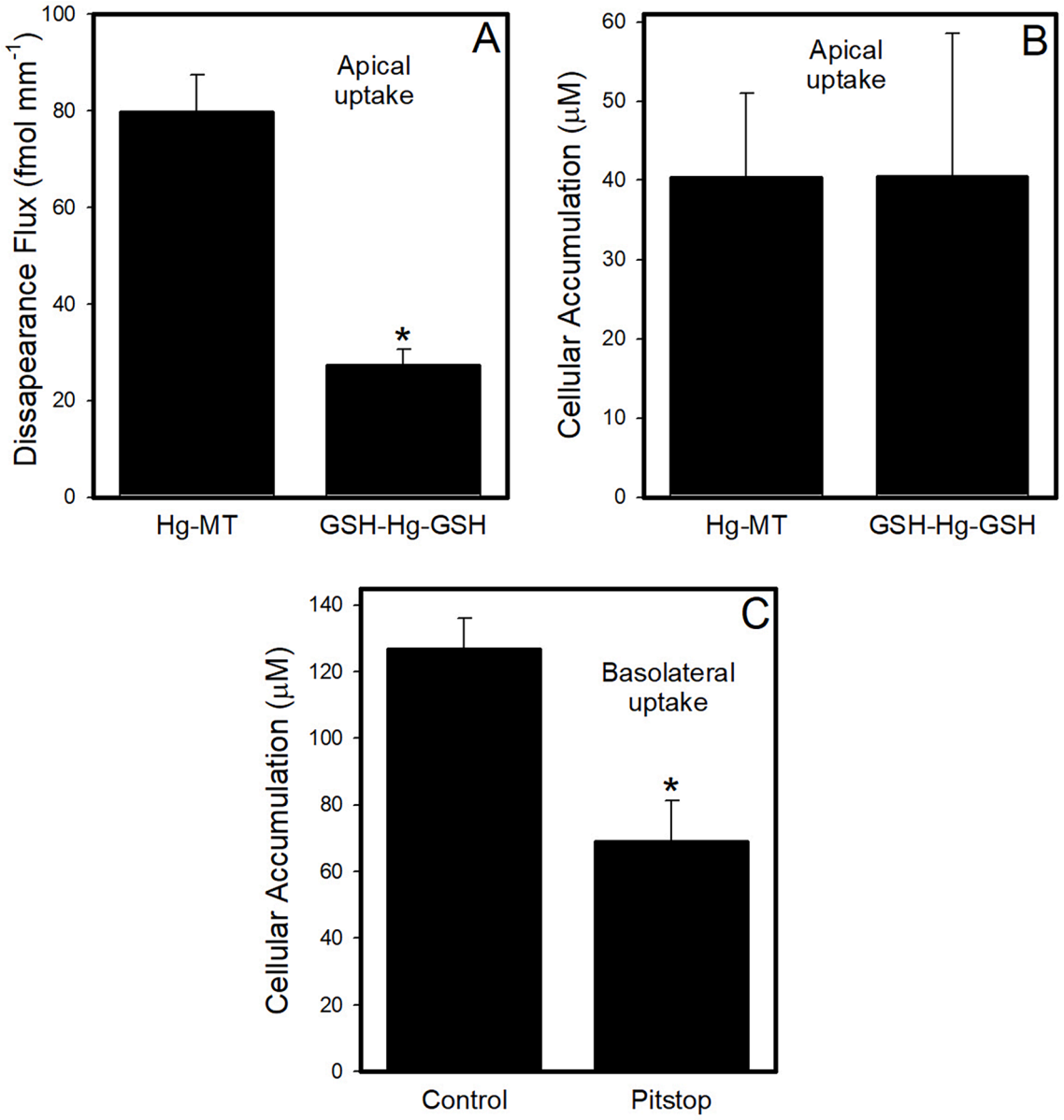

Fig. 11. Uptake of Hg-MT in Isolated Proximal Tubules. Isolated segments of perfused proximal tubules were used to measure the apical (luminal) uptake of Hg-MT complexes (A). The disappearance flux (J_D) measures disappearance of Hg-MT from the lumen and thus, represents transport across the apical membrane into the cell. The cellular accumulation (B) of Hg-MT was also analyzed in isolated proximal tubules perfused through the lumen to measure apical uptake. Basolateral uptake (C) of Hg-MT was measured in isolated, non-perfused proximal tubules treated with or without an inhibitor of endocytosis (Pitstop, 30 μM). n = 9. *, significantly different ($p < 0.5$) from the mean of the corresponding group.

Pittman: Investigation, Writing – review & editing. **Anasalea V.G. Caroland:** . **Jennifer Barkin:** Formal analysis, Writing – review & editing. **Christy C. Bridges:** Conceptualization, Formal analysis, Funding acquisition, Methodology, Project administration, Resources, Supervision, Writing – original draft, Writing – review & editing.

Declaration of Competing Interest

The authors declare that they have no known competing financial interests or personal relationships that could have appeared to influence the work reported in this paper.

Data availability

Data will be made available on request.

Acknowledgements

This work was supported by an NIH grant (ES030867) awarded to Dr. Bridges.

References

Agarwal, R., Raisuddin, S., Tewari, S., Goel, S.K., Raizada, R.B., Behari, J.R., 2010. Evaluation of comparative effect of pre- and posttreatment of selenium on mercury-induced oxidative stress, histological alterations, and metallothionein mRNA expression in rats. Journal of Biochemical and Molecular Toxicology 24, 123–135.

Agrawal, S., Flora, G., Bhatnagar, P., Flora, S.J., 2014. Comparative oxidative stress, metallothionein induction and organ toxicity following chronic exposure to arsenic, lead and mercury in rats. Cellular and Molecular Biology (Noisy-le-Grand, France) 60, 13–21.

Barfuss, D.W., Buchanan, J.T., Joshee, L., Pittman, E.H., D'Souza, N., Matta, K.E., Brownlee, R.T., Bridges, C.C., 2022. Hepatic processing of mercuric ions facilitates delivery to renal proximal tubules. Toxicology Letters 359, 1–9.

Belanger, M., Westin, A., Barfuss, D.W., 2001. Some health physics aspects of working with 203Hg in university research. Health Physics 80, S28–S30.
Bridges, C.C., Bauch, C., Verrey, F., Zalups, R.K., 2004. Mercuric conjugates of cysteine are transported by the amino acid transporter system b(0,+): implications of molecular mimicry. Journal of the American Society of Nephrology: JASN 15, 663–673.
Bridges, C.C., Zalups, R.K., Joshee, L., 2015. Toxicological significance of renal Bcrp: Another potential transporter in the elimination of mercuric ions from proximal tubular cells. Toxicol Appl Pharmacol 285, 110–117.
Bridges, C.C., Joshee, L., Zalups, R.K., 2008a. MRP2 and the DMPS- and DMSA-mediated elimination of mercury in TR(-) and control rats exposed to thiol S-conjugates of inorganic mercury. Toxicological Sciences 105, 211–220.
Bridges, C.C., Zalups, R.K., 2017. Mechanisms involved in the transport of mercuric ions in target tissues. Archives of Toxicology 91 (1), 63–81.
Bridges, C.C., Joshee, L., Zalups, R.K., 2008b. Multidrug resistance proteins and the renal elimination of inorganic mercury mediated by 2,3-dimercaptopropane-1-sulfonic acid and meso-2,3-dimercaptosuccinic acid. The Journal of Pharmacology and Experimental Therapeutics 324 (1), 383–390.
E.F. Carney Endocytosis in the proximal tubule Nat Rev Nephrol 15 1 2019 2 2.
Chan, H.M., Satoh, M., Zalups, R.K., Cherian, M.G., 1992. Exogenous metallothionein and renal toxicity of cadmium and mercury in rats. Toxicology 76, 15–26.
Cherian, M.G., Goyer, R.A., 1978. Role of metallothioneins in disease. Annals of Clinical and Laboratory Science 8, 91–94.
Dutta, D., Williamson, C.D., Cole, N.B., Donaldson, J.G., Rappoport, J.Z., 2012. Pitstop 2 is a potent inhibitor of clathrin-independent endocytosis. PLoS One1 7 (9).
Fujishiro, H., Sumino, M., Sumi, D., Umemoto, H., Tsuneyama, K., Matsukawa, T., Yokoyama, K., Himeno, S., 2022. Spatial localization of cadmium and metallothionein in the kidneys of mice at the early phase of cadmium accumulation. The Journal of Toxicological Sciences 47 (12), 507–517.
He, L., Xie, H., Bai, X.u., Zhao, J., Cui, L., Zhang, J., Li, B., Li, Y.-F., 2021. MALDI-TOF-MS and XAS analysis of complexes formed by metallothionein with mercury and/or selenium. Biometals 34 (6), 1353–1363.
Hossain, K.F.B., Hosokawa, T., Saito, T., Kurasaki, M., 2021. Zinc-pretreatment triggers glutathione and Nrf2-mediated protection against inorganic mercury-induced cytotoxicity and intrinsic apoptosis in PC12 cells. Ecotoxicology and Environmental Safety 207, 111320.
Lee, H.B., Blaufox, M.D., 1985. Blood volume in the rat. Journal of Nuclear Medicine 26, 72–76.
Ljubojevic, M., Orct, T., Micek, V., Karaica, D., Jurasovic, J., Breljak, D., Madunic, I.V., Rasic, D., Jovanovic, I.N., Peraica, M., Geric, M., Gajski, G., Oguic, S.K., Rogic, D., Nanic, L., Rubelj, I., Sabolic, I., 2019. Sex-dependent expression of metallothioneins MT1 and MT2 and concentrations of trace elements in rat liver and kidney tissues: Effect of gonadectomy. Journal of Trace Elements in Medicine and Biology 53, 98–108.
Merlos Rodrigo, M.A., Jimenez Jimemez, A.M., Haddad, Y., Bodoor, K., Adam, P., Krizkova, S., Heger, Z., Adam, V., 2020. Metallothionein isoforms as double agents - Their roles in carcinogenesis, cancer progression and chemoresistance. Drug Resistance Updates 52.
Mesquita, M., Pedroso, T.F., Oliveira, C.S., Oliveira, V.A., do, Santos,, R.F.,, Bizzi,, C.A.,, Pereira,, M.E.,, 2016. Effects of zinc against mercury toxicity in female rats 12 and 48 hours after HgCl2 exposure. EXCLI Journal 15, 256–267.
Nishimura, H., Nishimura, N., Tohyama, C., 1989. Immunohistochemical localization of metallothionein in developing rat tissues. The Journal of Histochemistry and Cytochemistry 37 (5), 715–722.
Nordberg, M., Nordberg, G.F., 2022. Metallothionein and Cadmium Toxicology-Historical Review and Commentary. Biomolecules 12 (3), 360.
Norseth, T., Clarkson, T.W., 1970a. Biotransformation of methylmercury salts in the rat studied by specific determination of inorganic mercury. Biochemical Pharmacology 19 (10), 2775–2783.
Norseth, T., Clarkson, T.W., 1970b. Studies on the biotransformation of 203Hg-labeled methyl mercury chloride in rats. Archives of Environmental Health 21 (6), 717–727.
Oliveira, V.A., de Souza da Costa, N., Mesquita, M., Pedroso, T.F., da Luz Fiuza, T., Peixoto, N.C., Pereira, M.E., Oliveira, C.S., 2020. Mercury toxicity in pregnant and lactating rats: zinc and N-acetylcysteine as alternative of prevention. Environmental Science and Pollution Research International 27 (32), 40563–40572.
Park, J.D., Liu, Y., Klaassen, C.D., 2001. Protective effect of metallothionein against the toxicity of cadmium and other metals(1). Toxicology 163, 93–100.
Piletz, J.E., Andersen, R.D., Berry, W., Herschman, H.R., 1983. Synthesis and degradation of hepatic metallothionein in mice differing in susceptibility to cadmium mortality. Biochemical Genetics 21 (5-6), 561–578.
Pittman, E.H., D'Souza, N., Mathis, T.N., Joshee, L., Barkin, J.L., Bridges, C.C., 2020. Sex differences in renal handling of inorganic mercury in aged rats. Curr Res Toxicol 1, 1–4.
Sabolic, I., Skarica, M., Ljubojevic, M., Breljak, D., Herak-Kramberger, C.M., Crljen, V., Ljubesic, N., 2018. Expression and immunolocalization of metallothioneins MT1, MT2 and MT3 in rat nephron. Journal of Trace Elements in Medicine and Biology 46, 62–75.
Who, 2020. chemicals of public health concern. World Health. Organization 10.
Wolff, N.A., Abouhamed, M., Verroust, P.J., Thévenod, F., 2006. Megalin-dependent internalization of cadmium-metallothionein and cytotoxicity in cultured renal proximal tubule cells. The Journal of Pharmacology and Experimental Therapeutics 318 (2), 782–791.
Zalups, R.K., Barfuss, D.W., 1996a. In Vitro Perfusion of Isolated Nephron Segments: A Method for Renal Toxicology. In: Zalups, R.K., Lash, L.H. (Eds.), Methods in Renal Toxicology. CRC Press, New York, New York, pp. 124–146.
Zalups, R.K., Barfuss, D.W., 1996b. In vitro perfusion of isolated nephron segments: A method for renal toxicology. In: Zalups, R.K., Lash, L.H. (Eds.), Methods in Renal Toxicology. CRC Press, New York, pp. 123–146.
Zalups, R.K., Koropatnick, J., 2000. Temporal changes in metallothionein gene transcription in rat kidney and liver: relationship to content of mercury and metallothionein protein. The Journal of Pharmacology and Experimental Therapeutics 295, 74–82.
Zhang, D., Jin, T., Xu, Y.Q., Lu, Y.F., Wu, Q., Zhang, Y.K., Liu, J., 2012. Diurnal-and sex-related difference of metallothionein expression in mice. Journal of Circadian Rhythms 10, 5.